T_2-Prepared SSFP Improves Diagnostic Confidence in Edema Imaging in Acute Myocardial Infarction Compared to Turbo Spin Echo

Peter Kellman,* Anthony H. Aletras, Christine Mancini, Elliot R. McVeigh, and Andrew E. Arai

T_2-weighted MRI of edema in acute myocardial infarction (MI) provides a means of differentiating acute and chronic MI, and assessing the area at risk of infarction. Conventional T_2-weighted imaging of edema uses a turbo spin-echo (TSE) readout with dark-blood preparation. Clinical applications of dark-blood TSE methods can be limited by artifacts such as posterior wall signal loss due to through-plane motion, and bright subendocardial artifacts due to stagnant blood. Single-shot imaging with a T_2-prepared SSFP readout provides an alternative to dark-blood TSE and may be conducted during free breathing. We hypothesized that T_2-prepared SSFP would be a more reliable method than dark-blood TSE for imaging of edema in patients with MI. In patients with MI (22 acute and nine chronic MI cases), T_2-weighted imaging with both methods was performed prior to contrast administration and delayed-enhancement imaging. The T_2-weighted images using TSE were nondiagnostic in three of 31 cases, while six additional cases rated as being of diagnostic quality yielded incorrect diagnoses. In all 31 cases the T_2-prepared SSFP images were rated as diagnostic quality, correctly differentiated acute or chronic MI, and correctly determined the coronary territory. Free-breathing T_2-prepared SSFP provides T_2-weighted images of acute MI with fewer artifacts and better diagnostic accuracy than conventional dark-blood TSE. Magn Reson Med 57:891–897, 2007. Published 2007 Wiley-Liss, Inc.†

Key words: MRI; heart; myocardial infarction; acute MI; edema; free-breathing; motion correction; parallel imaging

T_2-weighted MRI of edema in acute myocardial infarction (MI) provides a means of differentiating acute and chronic MI (1), and assessing the area at risk of infarction (2). Conventional T_2-weighted imaging of myocardial edema uses a turbo spin-echo (TSE) readout with dark-blood preparation (3). Dark-blood TSE methods are subject to artifacts such as posterior wall signal loss due to cardiac motion (4), and bright subencodcardial rims due to stagnant blood, which can significantly limit clinical use. Thus, the clinical application of T_2-weighted cardiac MR (CMR) is hindered by the poor reliability of standard methods (5).

The increase in T_2 associated with edema in acute MI may be relatively small (6), and the detection of changes in T_2-weighted signal intensity is challenging, particularly since the region of edema is generally not well delineated. It is therefore essential to have good signal uniformity across the heart. For this reason, surface-coil intensity correction is important. The use of dark-blood preparation used in TSE T_2-weighted imaging introduces potential signal loss due to through-plane cardiac motion, which is most noticeable in the posterior wall. In many cases, such signal loss causes an intensity variation that is indistinguishable from the increase in T_2 arising from edema, or it may cause normal myocardium to appear to have elevated T_2, resulting in a false-positive diagnosis. The effects of cardiac motion may be minimized by carefully choosing the timing of the TSE readout; however, this is difficult at higher heart rates, and is virtually impossible in cases of R-R variation. Cardiac wall motion and its effects on dark-blood TSE have been characterized in detail using labeling to track the motion (4). Optimizing the timing is an extra burden that complicates the exam.

Single-shot imaging with a T_2-prepared SSFP readout provides an alternative to dark-blood TSE and may be conducted during free-breathing. This is desirable when patients cannot tolerate breath-holding. Single-shot SSFP imaging has been employed for delayed-enhancement viability imaging (7–9), providing rapid coverage, immunity to arrhythmias, and elimination of breathing artifacts. Single-shot SSFP may be acquired with free breathing, and multiple images may be motion-corrected and averaged to enhance the signal-to-noise ratio (SNR) (8).

The current study used T_2-prepared single-shot SSFP with parallel imaging to reduce the imaging duration, and employed motion-corrected averaging to gain additional SNR. T_2-prepared SSFP image quality and diagnostic accuracy were tested in 22 patients with acute MI and nine patients with chronic MI.

MATERIALS AND METHODS

Study Protocol

Imaging was performed in patients and normal volunteers under clinical research protocols approved by the institutional review boards of the National Heart, Lung, and Blood Institute and Suburban Hospital, after the subjects provided informed consent. Acute MI was diagnosed on the basis of the clinical presentation, including symptoms, serum troponin, and coronary angiography. Chronic MI was defined as more than 1 year after a recognized acute

MI. The chronic-MI patients in this study did not have any recent symptoms or clinically recognized events.

The signal uniformity for T_2-weighted imaging using both dark-blood TSE and T_2-prepared single-shot SSFP was measured for normal volunteers ($N = 8$). A midventricular short-axis (SAX) slice was acquired using both methods. The timing of the readout for the TSE methods was optimized to minimize cardiac motion related signal loss. The difference in signal intensity between the septal and posterior LV wall regions was measured and compared for the two methods, after correcting for surface-coil intensity variation.

T_2-weighted imaging using both dark-blood TSE and T_2-prepared single-shot SSFP was performed on patients within 8 days of acute MI ($N = 22$) and more than 1 year after chronic MI ($N = 9$). The imaging protocol included localization, cardiac function using retrospectively gated cine SSFP, T_2-weighted imaging using both dark-blood TSE and T_2-prepared single-shot SSFP, and delayed-enhancement imaging using segmented phase-sensitive inversion recovery (PSIR) turbo fast low-angle shot (Turbo-FLASH) (10), typically 10 min following contrast agent administration (0.15 mmol/kg, Gd-DTPA, Magnevist; Berlex). Complete heart coverage in the SAX plane was obtained for all protocols. For acute-MI patients, there were 16 male and six female patients, with a mean age of 63.2 ± 11.1 years (mean ± SD). The time from the peak elevation in troponin was 3.6 ± 2 days (range = 1–8 days), and the peak troponin range had a mean of 34.4 ± 33.7 ranging from 0.94 to 116. For chronic MI, all patients were male, with a mean age of 69.8 ± 10.5 years (mean ± SD).

Cardiac Imaging

Experiments were conducted using a 1.5T Siemens Espree wide-bore imaging system using a custom pulse sequence and image reconstruction software. Raw data, including prescan noise and ECG waveforms, were acquired for all scans and images. Image reconstruction was performed both online for clinical use and offline from raw data using Matlab software (The Mathworks, Natick, MA, USA) in order to facilitate accurate SNR measurement (18).

A T_2-prepared single-shot SSFP sequence was used to repetitively acquire an interleaved T_2-weighted image and a reference image every two R-R intervals (Fig. 1). The T_2-weighted image and the reference image were obtained at the same phase of the cardiac cycle aiming for mid-diastole on sequential heartbeats using prospective ECG gating. A T_2 preparation was applied every second heartbeat prior to the SSFP readout for the T_2-weighted images. The reference image was used for estimating coil sensitivity maps for parallel imaging and surface-coil intensity correction. The reference image was acquired using a low-flip-angle gradient-echo (GRE) readout to provide a proton density (PD)-weighted image for surface-coil correction. Single-shot SSFP can be acquired with free breathing, and multiple images can be motion-corrected and averaged to enhance SNR (8). In this study, eight T_2-weighted images were acquired over 16 heartbeats. The subjects were instructed to hold their breath; however, significant motion was observed due to diaphragmatic drift or, in a few cases, the patient's inability to breath-hold. Motion correction
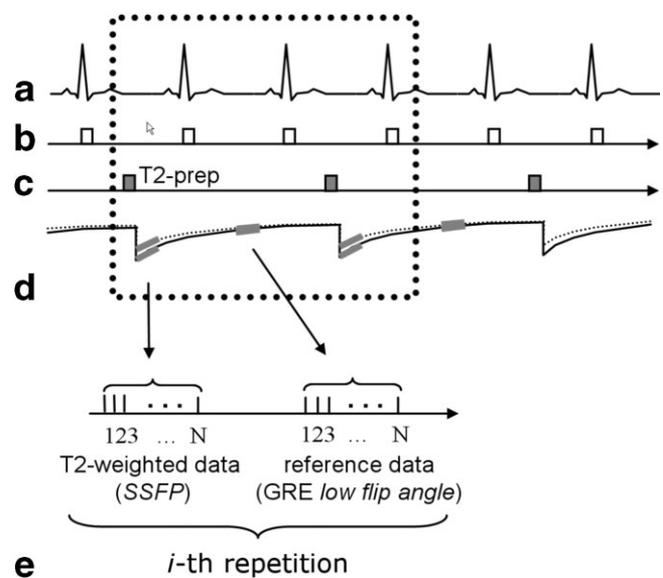
FIG. 1. Pulse sequence diagram for T_2-prepared single-shot SSFP imaging with acquisition of T_2-weighted data and reference data for B_1 maps used for parallel imaging autocalibration and surface-coil intensity correction: (**a**) ECG, (**b**) R-wave trigger, (**c**) T_2 preparation, (**d**) magnetization, and (**e**) data acquisition (during mid-diastole) for the i-th repetition.

used rigid body registration (8,11), and images were averaged to enhance SNR.

The T_2 preparation was an iterative Carr-Purcell Malcom-Levitt (MLEV) sequence (12–14) that consisted of a sequence of 90°x, 180°x, 180°x, −180°x, −180°x, −90°x RF pulses with overall duration TE followed by a gradient to spoil the transverse magnetization (RF pulses spaced TE/8, TE/4, TE/4, TE/4, TE/8). The 180° pulses were composite pulses (90°x, 180°y, 90°x) to provide more uniform off-resonance behavior (14). The final −90° tip-up pulse was a composite (270°x, −360°x) pulse as well. The T_2-weighted signal intensity exp($-TE/T_2$) was determined (to first order) by the T_2-preparation duration TE. In this study a TE of 60 ms was used.

The SSFP sequence used a run-up ($N = 10$ pulses) with linear ramp flip angle to reduce the transient magnetization during the interrupted steady-state approach (15). The reference image used a GRE readout with the same bandwidth as the SSFP readout and identical timing to the SSFP readout. The use of a low-flip-angle GRE readout for the reference image provided PD-weighted images and avoided fat-water cancellation, which can degrade the surface-coil intensity correction.

Parallel imaging (16) was used for acceleration by a factor of 2, by undersampling the phase encodes acquired for the T_2-weighted image. Typically, full resolution corresponded to 108–128 phase encodes depending on the phase field of view (FOV). The phase encodes acquired for the reference image were fully sampled at a lower (by one-half) resolution. The FOV of the reference image was two times that of the T_2-weighted image in order to ensure that there was no aliasing in the reference image used for computing the SENSE unmixing coefficients, and there-

FIG. 2. Acute-MI patient exhibiting edema in the LAD territory with true-positive imaging by both dark-blood TSE (left) and T_2-prepared SSFP (center). The delayed enhancement is shown at right. Arrows indicate regions of increased intensity.
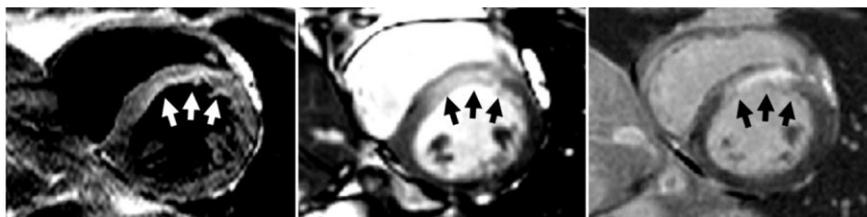
fore the spatial resolution of the reference was one-quarter that of the T_2-weighted image. Prescan noise was acquired to calculate noise statistics used for optimal array combining (10,17). The surface-coil intensity variation was corrected by dividing the T_2-weighted image with the median filtered reference magnitude image (10).

Dark-blood TSE imaging used an ECG-gated segmented sequence with a double inversion-recovery (DIR) preparation applied immediately following the ECG trigger, and TSE readout in diastole timed to minimize cardiac motion. ECG triggering used two R-R intervals between readouts. The dark-blood preparation used a selective component that was 300% of the 6-mm slice thickness used for imaging. Surface-coil intensity correction was performed using a low-resolution PD-weighted dataset acquired during a prescan calibration.

For both sequences, the in-plane resolution was typically 1.9×2.5 mm² with 6-mm slice thickness (typical matrix size = 192×108) and rectangular FOV (75%). TSE images used a bandwidth = 449Hz/pixel, echo-train length = 25, echo spacing = 4.96 ms, and effective TE = 64 ms, with a 124-ms imaging duration. Single-shot T_2-prepared SSFP images used a bandwidth = 977 Hz/pixel, TE/TR = 1.6/3.2 ms, flip angle = 90°, and T_2-preparation TE = 60 ms. Parallel imaging (rate 2) was used to obtain the full phase-encode resolution with an imaging duration of 173 ms in the cardiac cycle. The T_2-prepared SSFP imaging sequence used a low-flip-angle GRE readout with 5° readout flip angle for the PD reference image. All images were acquired using 12 surface-coil elements (six anterior and six posterior; Siemens product coils).

Delayed-enhancement imaging was performed using a PSIR segmented TurboFLASH sequence (10). Typical imaging parameters for delayed-enhancement imaging were bandwidth = 140 Hz/pixel, TE/TR = 4.2/8.7 ms, readout flip angle = 25°, FOV = 360×370 mm², in-plane spatial resolution = 1.4×2.2 mm² (matrix = 256×125), views per segment = 25, and slice thickness = 6 mm.

Measurements

The uniformity of T_2-weighted signal intensity in the myocardium was quantified by comparing the mean intensity in septal and posterior wall regions for eight normal volunteers. All images were corrected for surface-coil intensity variation; therefore, a uniform T_2-weighted signal intensity should be expected.

Delayed-enhancement images for the acute-MI patients were used to determine the coronary territory involvement. The coronary territory corresponding to the region with elevated T_2 was determined for each approach blinded to the clinical history or the delayed-enhancement images. The coronary territories determined to have edema on each type of T_2-weighted image were then compared with the territories with MI to determine the diagnostic accuracy. Images for chronic-MI cases were mixed with acute-MI cases and assessed at the same time. In the case of chronic MI, regions with apparent elevated T_2 were scored as false positives.

SNR measurements were made using images reconstructed in SNR units (18) using prescan noise. SNR measurements were made on uniform noise images, i.e, prior to surface-coil intensity correction. The SNR was measured in the same region of interest (ROI) for both methods; therefore, surface-coil variation affected the contrast-to-noise ratio (CNR) in the same way for both methods. For normal volunteers the SNR was always measured in the same general location (septal region) to reduce variation due to surface-coil intensity. For acute-MI patients the SNR was measured in the edema region with elevated T_2 and in a remote region on the opposite wall. The CNR was calculated as the difference between the SNR for edema
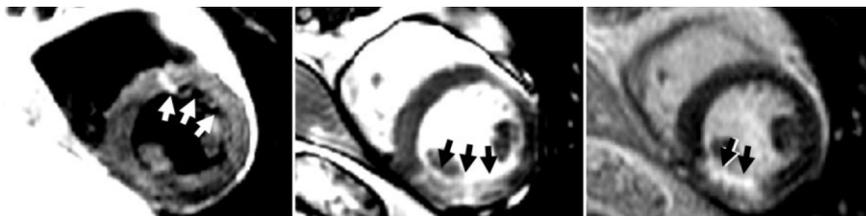
FIG. 3. Acute-MI patient exhibiting edema with false-positive dark-blood TSE (left) showing apparently elevated T_2 in the LAD (incorrect) coronary territory but true-positive T_2-prepared SSFP (center) with elevated-T_2 in the RCA territory. The delayed enhancement shown at right is consistent with an MI in the RCA territory. This patient had significant RR variability. Arrows indicate regions of increased intensity.
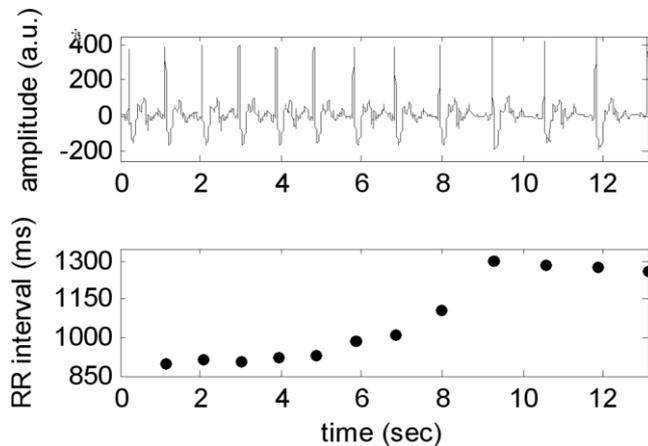
FIG. 4. ECG waveform and corresponding R-R interval exhibiting significant R-R variation during a breath-hold for a patient corresponding to images shown in Fig 3. The R-R interval increased from 900 to 1305 ms.

and that for remote regions. Statistical significance was determined by paired t-test.

RESULTS

Normal Volunteers

In normal volunteers ($N = 8$), in whom uniform T_2-weighted signal intensity was expected, the loss in signal intensity of the posterior wall of the LV (midventricular SAX slice) compared to the septal wall was 22.6% $\pm$ 13.7% (mean $\pm$ SD) using TSE, and 0.6% $\pm$ 4.2% using T_2-prepared SSFP. Both methods had surface-coil intensity correction, and TSE images used timing optimized for minimal cardiac motion. A signal loss of 23% would represent a large fraction of the expected difference in signal intensity between acute MI and normal myocardium (see Discussion).

The SNR in the septal region was 96.5 $\pm$ 9.2 (mean $\pm$ SD) using TSE, and 54.4 $\pm$ 10.7 (mean $\pm$ SD) using T_2-prepared SSFP ($P < 0.05$, $N = 8$).

Acute-MI Patients

In patients with acute MI ($N = 22$), T_2-weighted imaging with both methods was performed prior to contrast admin-istration and delayed-enhancement imaging of viable myo-cardium. In all 22 cases the T_2-prepared SSFP was rated to be of diagnostic quality and yielded the correct diagnosis (i.e., 100% agreement with coronary territory involvement as determined from delayed-enhancement images). The MI territory was determined to correspond to the left anterior descending (LAD) coronary artery in 10 patients, to the right coronary artery (RCA) in 10 patients, and to the circumflex in two patients. In the Fig. 2 example, the elevated T_2 regions for both the dark-blood TSE and T_2-prepared SSFP images are in agreement with the antero-septal MI evident in the delayed-enhancement image.

The T_2-weighted images using TSE were nondiagnostic in three of 22 cases, while one additional case (Fig. 3) that was rated to be of diagnostic quality had incorrect diagnosis (incorrect coronary territory). The case of Fig. 3 corresponds to a patient with significant R-R variation during the breath-hold, as seen in the ECG waveform (Fig. 4). In this case the TSE image (left) has a false-positive apparent elevation of T_2 in the LAD coronary distribution on images independently judged to be of diagnostic quality. However, the T_2-prepared SSFP (center) with elevated-T_2 in the RCA territory yielded the correct diagnosis and is in agreement with the delayed-enhancement image (right) with an MI in RCA territory. In a third example (Fig. 5), the dark-blood TSE image (left) was judged to be nondiagnostic. The T_2-prepared SSFP (center) and delayed-enhancement image (right) are in agreement with MI in the LAD territory.

The SNR in the region of elevated T_2 was 89.3 $\pm$ 28.6 (mean $\pm$ SD) using TSE, and 73.2 $\pm$ 16.6 using T_2-prepared SSFP ($P < 0.05$, $N = 21$), and 64.3 $\pm$ 24.4 and 45.8 $\pm$ 14.0 ($P < 0.05$, $N = 21$) in the remote zone for TSE and T_2-prepared SSFP, respectively. The measured CNR between the region of elevated T_2 and remote zone was 25.0 $\pm$ 25.1 for TSE and 27.4 $\pm$ 19.6 for T_2-prepared SSFP ($P = 0.53$, not significant). SNR was measured in 21 of 22 acute MI patients since the raw data for one patient were not saved.

The average heart rate was 61.4 $\pm$ 11.9 beats per minute (bpm; mean $\pm$ SD) ranging from 48 to 89 bpm. The RR variation for two out of three of the nondiagnostic TSE cases and the case with incorrect diagnosis was >100 ms, and these patients had a mean heart rate of 73 bpm.

Chronic-MI Patients

Chronic-MI patients ($N = 9$) were imaged according to the same protocol used for the acute-MI patients. The MI ter-
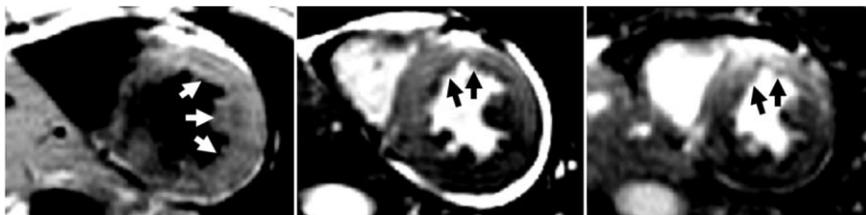
FIG. 5. Acute-MI patient exhibiting edema in the LAD coronary territory with a nondiagnostic dark-blood TSE image but true-positive T_2-prepared SSFP image. The dark-blood TSE (left) was considered to be nondiagnostic with apparent elevated T_2 spanning two coronary territories. The T_2-prepared SSFP (center) showed elevated T_2 in the LAD territory, in agreement with delayed enhancement (right). Arrows indicate regions of increased intensity.

FIG. 6. Patient with chronic MI in the RCA territory is negative for edema with both dark-blood TSE and T$_2$-prepared SSFP in agreement. Left: dark-blood TSE; center: T$_2$-prepared SSFP; right: delayed enhancement. Images are surface-coil intensity-corrected. Arrows indicate regions of increased intensity.
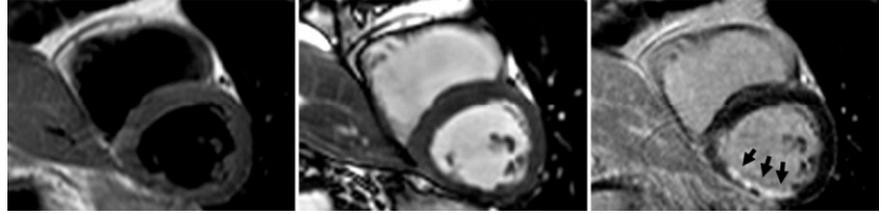
ritories included two in the LAD distribution and seven in RCA distribution. In all nine cases the T$_2$-prepared SSFP was rated to be of diagnostic quality and yielded the correct diagnosis (i.e., no apparent edema). In the case of dark-blood TSE, there were five false-positive cases with apparent edema, with three suggesting abnormalities in the LAD territory and two in both the LAD and RCA territories. Example images for chronic MI are shown for cases with correct diagnosis (Fig. 6) and a false-positive case (Fig. 7).

In summary (Fig. 8), the dark-blood TSE method was found to provide diagnostic quality imaging with a correct diagnosis in only 72% of the cases (acute and chronic combined) while the T$_2$-prepared SSFP was of diagnostic quality and correct in 100% of the patients.

The average heart rate was 57.4 ± 9.8 bpm (mean ± SD) ranging from 43 to 69 bpm. The five false-positive cases had mean heart rate of 59 bpm, and the RR variation ranged from 20 to 75 ms.

DISCUSSION

T$_2$-prepared SSFP had higher diagnostic accuracy than T$_2$-prepared dark-blood TSE with respect to determining the coronary artery distribution and determining whether a patient had an acute or chronic MI. In this study, relying on dark-blood TSE images yielded correct diagnoses in 82% of patients with acute MI and only 44% for chronic MI, while the T$_2$-prepared SSFP images had 100% diagnostic accuracy. With dark-blood TSE, most of the incorrect cases could be attributed to signal loss caused by through-plane cardiac motion. The higher percentage of false-positive TSE images for the chronic MI cases was partially due to a larger number of patients with arrhythmia or large RR variation. In this study the reference standard for determining the correct assessment of edema in acute MI was based on correlation with delayed enhancement, which was compatible with the clinical presentation, including coronary angiography.

The expected difference in T$_2$-weighted signal intensity (exp(–TE/T$_2$)) between acute MI and normal myocardium is estimated to be on the order of 25–50% for T$_2$ in range 45–50 ms for normal myocardium and 60–65 ms for acute MI. Therefore, signal uniformity is of paramount importance for detection of relatively small changes in T$_2$ expected for edema. Signal uniformity is critical for determination of the size of elevated T$_2$ region. In this regard, correction of surface-coil intensity variation is very important. Signal loss due to through-plane cardiac motion in dark-blood prepared TSE imaging reduces the reliability of this method, and while this may be mitigated to some extent by adjusting the timing of readout, it is difficult to achieve the desired level of reliability, particularly in a clinical setting with higher heart rates and significant R-R variability.

The T$_2$-prepared SSFP approach was sensitive to small changes in T$_2$ and had uniform signal intensity. SSFP off-resonance banding artifacts were not found to be a problem, although good shimming is desirable. Fat saturation was not used in the current study and on some occasions fat-water cancellation (particularly epicardial fat) led to dark voxels in the border between fat and myocardium due to a partial-volume effect. This could be avoided by slight center frequency adjustment (typically 50 Hz) without degrading the water signal. Importantly, unlike the signal loss in dark-blood TSE, the fat-water cancellation was easily distinguishable and could be read through, not leading to a false result. The further reduction of TR or the introduction of fat saturation would improve this situation.

The SNR of dark-blood TSE was significantly higher than the T$_2$-prepared SSFP due to a number of factors, such as the readout flip angle, bandwidth, and parallel imaging loss. However, our analysis indicates that signal unifor-
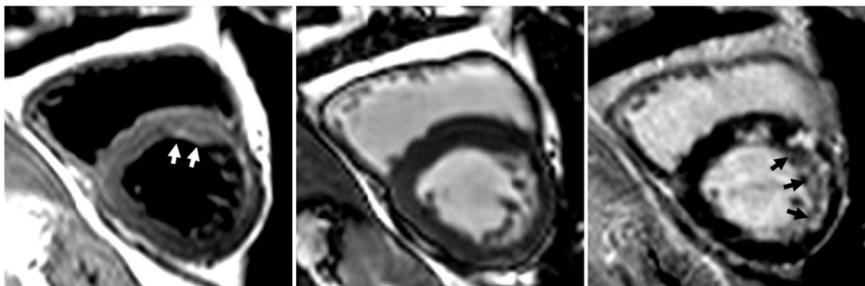
FIG. 7. Patient with chronic MI in the LAD territory showing a false-positive dark-blood TSE (left) suggesting edema, but true-negative T$_2$-prepared TSE (center). Delayed-enhancement images are at right. Images are surface-coil intensity-corrected. Arrows indicate regions of increased intensity.
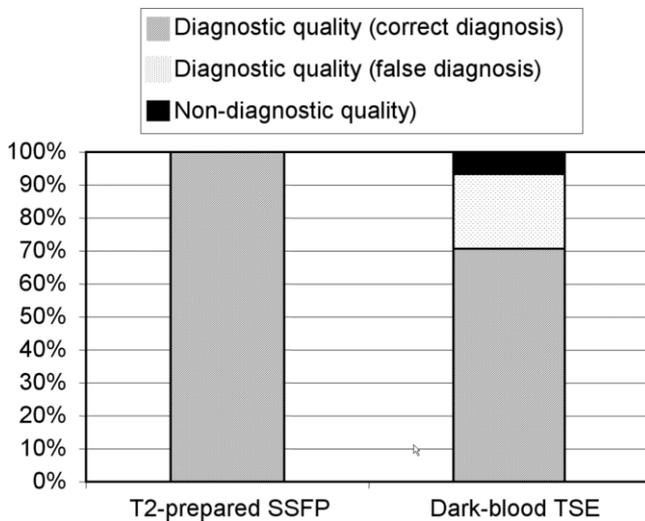
FIG. 8. Overall results for patients ($N = 31$) with both acute ($N = 22$) and chronic ($N = 9$) MI.

mity limits accurate detection and diagnosis of acute MI—not necessarily the SNR. Given the fact that TSE has higher SNR, it would be expected that the CNR between edema and remote regions would be correspondingly higher since the TE used to set the T_2-weighted contrast was approximately the same. However, the CNR for the T_2-prepared SSFP was approximately the same as the TSE, implying that either the T_2-weighted contrast for the TSE was reduced or the cardiac motion-related signal losses contributed to a loss of contrast. The T_2-weighted contrast mechanism for TSE relies on adjusting the TE, which is determined by the phase-encode order, whereas the T_2-prepared SSFP sequence determines the TE in the T_2-preparation and uses a linear phase-encode order. The TSE method used a product sequence with TSE parameters selected approximately the same as in prior literature (1,2). It is also noted that the SNR and CNR measurements in this paper were calculated by convention using the noise SD, which differs from the previous reported (1,2) definition using mean noise. While the mean and SD are related for a given noise distribution, the SD is a more meaningful statistic for predicting detectability and is preferable to the mean, which depends on the number of receive coil elements.

Stagnant blood along the endocardial surface is another source of artifact in dark-blood TSE imaging (Fig. 9). While arguably the blood rims might be discriminated from myocardium using other images to define the endocardial border, this requires perfect breath-hold registration and adds complexity. These artifacts can further confound assessment of the size of edema regions. Although none of the false-positive cases in this study were attributed to this artifact, such artifacts may reduce the confidence particularly for apical slices. The bright signals also create a dilemma in image display since it is difficult to set a grayscale that properly covers normal myocardium, the slightly brighter acute MI, and the much brighter blood near the endocardium.

Increasing the imaging slice thickness (e.g., to 15 mm (1,4)) and commensurately increasing the dark-blood preparation slice thickness will reduce the effects of cardiac motion-related signal loss for dark-blood prepared TSE. The 6-mm slice thickness used in this comparison may have somewhat reduced the diagnostic accuracy of the dark-blood TSE. However, increasing the slice thickness also increases the stagnant-blood artifact (4). Since the T_2-prepared SSFP method does not have either of these artifacts, which are caused by the dark-blood preparation, the T_2-prepared SSFP is a more robust method. The sensitivity for detection of edema with increased slice thickness will not be significantly reduced in cases with large size regions of edema. However, thicker slices will have reduced sensitivity for detecting focal areas of edema that may result in cases such as acute myocarditis or sarcoidosis (4). In cases with a large region of edema, an increased slice thickness would improve the SNR for both dark-blood TSE and T_2-prepared SSFP methods.

CONCLUSIONS

The proposed T_2-prepared SSFP bright-blood approach overcomes artifacts such as posterior wall signal loss due to cardiac motion, and bright subendocardial rims due to stagnant blood. T_2-prepared SSFP resolves two artifact mechanisms that significantly limit the widely used dark-blood TSE methods. The TSE method was sensitive to variations in RR and image quality suffered at higher heart rates, whereas the single-shot T_2-prepared SSFP approach was robust to such variation and enabled non-breath-hold imaging. T_2-prepared SSFP may be used clinically for reliable T_2-weighted imaging in acute MI.
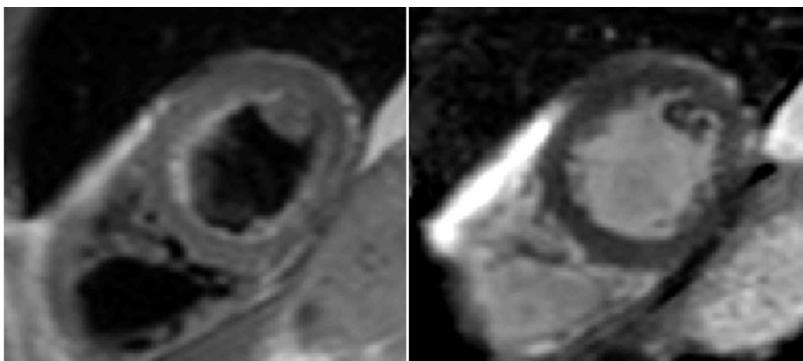
FIG. 9. Example illustrating bright-blood artifact for dark-blood TSE image (left) resulting from stagnant blood within trabeculae along endocardial wall. The corresponding T_2-prepared SSFP image (right) has no blood artifact.

REFERENCES

1. Abdel-Aty H, Zagrosek A, Schulz-Menger J, Taylor AJ, Messroghli D, Kumar A, Gross M, Dietz R, Friedrich MG. Delayed enhancement and T2-weighted cardiovascular magnetic resonance imaging differentiate acute from chronic myocardial infarction. Circulation 2004;109:2411–2416.

2. Aletras AH, Tilak GS, Natanzon A, Hsu LY, Gonzalez FM, Hoyt Jr RF, Arai AE. Retrospective determination of the area at risk for reperfused acute myocardial infarction with T2-weighted cardiac magnetic resonance imaging: histopathological and displacement encoding with stimulated echoes (DENSE) functional validations. Circulation 2006; 113:1865–1870.

3. Simonetti OP, Finn JP, White RD, Laub G, Henry DA. "Black blood" T2-weighted inversion-recovery MRI of the heart. Radiology 1996;199: 49–57.

4. Keegan J, Gatehouse PD, Prasad SK, Firmin DN. Improved turbo spin-echo imaging of the heart with motion-tracking. J Magn Reson Imaging 2006;24:563–570.

5. Pennell D. Myocardial salvage: retrospection, resolution, and radio waves. Circulation 2006;113:1821–1823.

6. Wisenberg G, Prato FS, Carroll SE, Turner KL, Marshall T. Serial nuclear magnetic resonance imaging of acute myocardial infarction with and without reperfusion. Am Heart J 1988;115:510–518.

7. Chung Y, Vargas J, Simonetti O, Kim R, Judd R. Infarct imaging in a single heart beat. J Cardiovasc Magn Reson 2002;4:12–13.

8. Kellman P, Larson AC, Hsu LY, Chung YC, Simonetti OP, McVeigh ER, Arai AE. Motion-corrected free-breathing delayed enhancement imaging of myocardial infarction. Magn Reson Med 2005;53:194–200.

9. Huber A, Schoenberg SO, Spannagl B, Rieber J, Erhard I, Klauss V, Reiser MF. Single-shot inversion recovery TrueFISP for assessment of myocardial infarction. AJR Am J Roentgenol 2006;186:627–633.

10. Kellman P, Arai AE, McVeigh ER, Aletras AH. Phase-sensitive inversion recovery for detecting myocardial infarction using gadolinium-delayed hyperenhancement. Magn Reson Med 2002;47:372–383.

11. Thevenaz P, Ruttimann UE, Unser M. A pyramid approach to subpixel registration based on intensity. IEEE Trans Image Process 1998;7:27–41.

12. Brittain JH, Hu BS, Wright GA, Meyer CH, Macovski A, Nishimura DG, Coronary angiography with magnetization-prepared T2 contrast. Magn Reson Med 1995; 33:689–96.

13. Shea SM, Deshpande VS, Chung YC, Li D. Three-dimensional True-FISP imaging of the coronary arteries: improved contrast with T2-preparation. J Magn Reson Imaging 2002;15:597–602.

14. Levitt M, Freeman R, Frenkiel T. Supercycles for broadband heteronuclear decoupling. J Magn Reson 1982;50:157–160.

15. Deshpande VS, Chung YC, Zhang Q, Shea SM, Li D. Reduction of transient signal oscillations in True-FISP using a linear flip angle series magnetization preparation. Magn Reson Med 2003; 49:151–157.

16. Pruessmann KP, Weiger M, Scheidegger MB, Boesiger P. SENSE: sensitivity encoding for fast MRI. Magn Reson Med 1999;42:952–962.

17. Roemer PB, Edelstein WA, Hayes CE, Souza SP, Mueller OM. The NMR phased array. Magn Reson Med 1990;16:192–225.

18. Kellman P, McVeigh ER. Image reconstruction in SNR units: a general method for SNR measurement. Magn Reson Med 2005;54:1439–1447.